Regulation of cytoskeletal mechanics and cell growth by myosin light chain phosphorylation

SHUANG CAI,[1] LIDIJA PESTIC-DRAGOVICH,[1] MARTHA E. O'DONNELL,[2] NING WANG,[3] DONALD INGBER,[4] ELLIOT ELSON,[5] AND PRIMAL DE LANEROLLE[1]

[1]*Department of Physiology and Biophysics, University of Illinois at Chicago, Chicago, Illinois 60612-7342;* [2]*Department of Human Physiology, University of California, Davis, California 95616-8644;* [3]*Physiology Program, Harvard University School of Public Health, Boston, 02115-6021;* [4]*Departments of Pathology and Surgery, Children's Hospital and Harvard University Medical School, Boston, Massachusetts 02116-5737; and* [5]*Department of Biophysics and Molecular Biophysics, Washington University Medical School, St. Louis, Missouri 63110-1093*

Cai, Shuang, Lidija Pestic-Dragovich, Martha E. O'Donnell, Ning Wang, Donald Ingber, Elliot Elson, and Primal de Lanerolle. Regulation of cytoskeletal mechanics and cell growth by myosin light chain phosphorylation. *Am. J. Physiol.* 275 (*Cell Physiol.* 44): C1349–C1356, 1998.—The role of myosin light chain phosphorylation in regulating the mechanical properties of the cytoskeleton was studied in NIH/3T3 fibroblasts expressing a truncated, constitutively active form of smooth muscle myosin light chain kinase (tMK). Cytoskeletal stiffness determined by quantifying the force required to indent the apical surface of adherent cells showed that stiffness was increased twofold in tMK cells compared with control cells expressing the empty plasmid (Neo cells). Cytoskeletal stiffness quantified using magnetic twisting cytometry showed an ~1.5-fold increase in stiffness in tMK cells compared with Neo cells. Electronic volume measurements on cells in suspension revealed that tMK cells had a smaller volume and are more resistant to osmotic swelling than Neo cells. tMK cells also have smaller nuclei, and activation of mitogen-activated protein kinase (MAP kinase) and translocation of MAP kinase to the nucleus are slower in tMK cells than in control cells. In tMK cells, there is also less bromodeoxyuridine incorporation, and the doubling time is increased. These data demonstrate that increased myosin light chain phosphorylation correlates with increased cytoskeletal stiffness and suggest that changing the mechanical characteristics of the cytoskeleton alters the intracellular signaling pathways that regulate cell growth and division.

cell stiffness; osmotic swelling; volume regulation; mitogen-activated protein kinase activation; cell division; myosin light chain kinase

THE ABILITY OF THE cytoskeleton to deform and reform is a crucial aspect of many cellular responses, such as cell motility and cell division (4). Migrating cells continuously change their cytoskeleton, and preventing these cytoskeletal changes by affecting actin polymerization or myosin II phosphorylation inhibits cell motility (47). A plastic cytoskeleton is also essential for proper progression through the cell cycle. Specific cytoskeletal alterations are required for a cell to enter S phase (20), and disrupting actin filaments prevents S phase entry and blocks mitosis (4, 32, 50). In addition, exposure to growth factors results in the stimulation of the mitogen-activated protein kinase (MAP kinase) pathway and cytoskeletal changes (20, 25), both of which are needed for a cell to commit to mitosis (25). Other experiments have shown that stabilizing microtubules blocks mitosis (39) and that inhibiting myosin II activity blocks cytokinesis (10, 26). Thus many cellular responses depend on the ability of the cytoskeleton to restructure itself.

The organization and, hence, the plasticity of the cytoskeleton is determined primarily by the forces or tension generated within the cytoskeleton by actin and myosin II (12, 23, 29, 39). The actin-myosin II interaction in smooth muscle and nonmuscle cells is regulated by the phosphorylation of the 20-kDa light chain of myosin by the enzyme myosin light chain kinase (MLCK) (1, 44). MLCK is naturally a calcium/calmodulin-dependent enzyme (1, 44). Proteolytic digestion (22) or insertion of a stop codon (19) between the catalytic and regulatory domains results in a truncated, constitutively active enzyme. Expression of the truncated catalytic domain of MLCK (tMK) in 3T3 cells increases myosin light chain phosphorylation (33). Therefore, to further characterize the relationship between cytoskeletal plasticity and cellular responses, we quantified the mechanical properties of the cytoskeleton, MAP kinase activation, and cell growth in NIH/3T3 cells expressing tMK or the empty plasmid.

MATERIALS AND METHODS

Cell culture. NIH/3T3 fibroblasts were transduced with either the pLNCX Moloney murine leukemia virus-based vector (a gift from A. Dusty Miller) or the same vector engineered to contain tMK. In this vector, the neomycin resistance gene is driven from the viral long terminal repeat, and the cloned genes are driven from the cytomegalovirus promoter. The tMK gene was constructed by inserting a stop codon following Lys-793 of the chicken gizzard smooth muscle MLCK gene (19). The 1995-bp tMK gene was passed through pBluescript and cloned into the pLNCX vector. The pLNCX and pLNCX-tMK DNA were then used to transfect GP+envAM12 amphotropic packaging cells. The packaging cells were then selected in G418 and expanded in culture. Medium from packaging cells in log phase growth, which contains infective viral particles, was then used to infect NIH/3T3 cells. Infected cells were selected for 8 days in 0.9 mg/ml G418 (effective concentration), expanded in culture, and used in the experiments described. Vector construction, generation of packaging cells, and infection and selection of

The costs of publication of this article were defrayed in part by the payment of page charges. The article must therefore be hereby marked "*advertisement*" in accordance with 18 U.S.C. Section 1734 solely to indicate this fact.

NIH/3T3 cells are described in detail in Ref. 33. Cells transduced with the neomycin resistance gene alone (Neo cells) and tMK cells were grown in DMEM containing 10% fetal bovine serum (FBS) and antibiotics at 37°C in an atmosphere containing 5% CO_2.

Myosin light chain phosphorylation. Neo or tMK cells grown in 60-mm dishes were washed in phosphate-free DMEM and incubated with 50 μCi of ^{32}P in 1 ml of phosphate-free DMEM for 6 h at 37°C. The cells were then washed with ice-cold PBS, frozen on dry ice, and extracted in 1% NP-40, 40 mM sodium pyrophosphate, 100 mM NaF, 500 mM NaCl, 10 mM EGTA, 5 mM EDTA, 50 μg/ml leupeptin, 50 μg/ml pepstatin, and 25 mM Tris (pH 7.9). The supernatant was collected by centrifugation (50,000 *g*, 20 min) and incubated with 10 μg of affinity-purified antibody to macrophage myosin II for 2 h, followed by incubation with protein A-Sepharose for 1.5 h. The beads were then washed extensively, and the myosin II-antibody complexes were eluted by boiling in 0.25% SDS, 5 mM dithiothreitol (DTT), and 5 mM Tris (pH 6.8). The immunoprecipitates were then analyzed by SDS-PAGE and autoradiography.

Quantification of cytoskeletal stiffness. Mechanical deformation assays were performed as described by Worthen et al. (49). Cells were plated on coverslips coated with 15 μg/ml poly(2-hydroxyethyl methacrylate) and allowed to attach for 4–6 h. The coverslips were then mounted in the chamber of the cell poker in the inverted position. Stiffness measurements were performed in degassed medium containing FBS at 37°C. The surface of the cells was indented near the center (depth of indentation was <2.6 μm and velocity of indentation was 5.1 μm/s) with a glass microprobe (tip diameter ~ 2 μm) attached to a flexible glass beam of known bending constant. The degree of bending of the glass beam is used to calculate cellular deformability (i.e., stiffness), which is the force resisting indentation (in millidynes) per unit of indentation depth (in micrometers), as described by Worthen et al. (49). Some cells were pretreated with okadaic acid for 10 min at 37°C or with okadaic acid for 10 min followed by cytochalasin D for 10 min at 37°C. Deformation assays were then performed for a maximum of 30 min at 37°C in the continued presence of the drugs.

Magnetic twisting cytometry (21, 46) was performed on cells grown in 96-well dishes. The resistance to twisting of beads coated with RGD peptides, in the presence or absence of 3 μM cytochalasin D, and of beads coated with acetylated low-density lipoproteins (AcLDL) was tested. Briefly, $\sim 2 \times 10^4$ ferromagnetic beads coated with RGD peptide or AcLDL were added to each well and incubated for 10–20 min at 37°C. Unbound beads were removed by washing in serum-free medium, and the cells were placed within the magnetometer and maintained at 37°C. The beads were then magnetized with a 1,000-gauss pulse so that their magnetic moments were aligned in one direction. A second magnetic field (26 gauss) that was too weak to remagnetize the beads was applied orthogonally to the original field. The beads rotated to reorient their magnetic moments with the new field. Changes in the component of the remanent magnetic field generated by the beads in the original direction were measured by an in-line magnetometer and reflect bead rotation. The rotation of RGD-coated beads is resisted by the cytoskeleton and is inversely proportional to the stiffness of the cytoskeleton. The stiffness was defined as the ratio of the applied stress to the measured bead rotation (strain).

Quantification of responses to changes in osmolarity. The responses of cells in monolayer to decreasing osmolarity was determined using an ECIS Biosensor (17). Cells were plated in a modified 96-well tissue culture plate containing a 10^{-3} cm^2 gold electrode and a large counter electrode. A 1-μA current was applied between the gold and counter electrodes, and the voltage was monitored using a lock-in amplifier. As cells attach, spread, and make cell-cell contacts, the insulating cell bodies block the current path and the resistance increases. The increase in resistance is a function of cell thickness and the integrity of the cell contacts, and changes in resistance reflect changes in cell morphology. The effect of changing osmolarity was determined by first equilibrating the cells in HEPES-buffered Hanks' salt solution (290 mosM; 20 mM HEPES). After baseline resistance measurements, the osmolarity was adjusted by sequentially replacing one-half of the medium bathing the cells with (in mM) 5.5 KCl, 1 $CaCl_2$, 1 $MgSO_4$, and 20 HEPES (pH 7.4) every 10 min, and the resistance was measured continuously.

The responses of cells in suspension to decreasing osmolarity were determined by performing electronic cell sizing (34). Cells were removed from the tissue culture plates by brief typsinization and washed and resuspended at 5×10^4 cells/ml in HEPES-buffered Hanks' salt solution (290 mosM; 20 mM HEPES) and were maintained at 37°C throughout the experiment. The osmolarity of the cells in suspension was adjusted by sequentially diluting the isosmotic solution with a hyposmotic solution consisting of (in mM) 5.5 KCl, 1 $CaCl_2$, 1 $MgSO_4$, and 20 HEPES (pH 7.4). Cell volumes were measured using a Coulter counter (model ZM) with a Coulter channelizer (C-1000). Absolute cell volumes were calculated from distribution curves of cell diameter, using a standard curve generated by polystyrene latex beads of known diameter (9.97 and 14.51 μm).

Measurement of nuclear sizing. Relative nuclear size was determined by performing flow cytometry on cells synchronized by growing them in 0.5% FBS for 48 h. The cells were then harvested, fixed, permeabilized, stained with propidium iodide (45), and analyzed for their DNA content using a Coulter EPICS Elite ESP flow cytometer. The pulse width of the fluorescence peak (time of flight) was used to obtain relative nuclear size. Nuclear size was measured three times, but only the data from a single experiment are reported. The time of flight is a relative measurement, and there is substantial interexperiment variability due to variability in the binding of propidium iodide to the DNA. Therefore, in each experiment, the Neo and tMK cells were incubated with propidium iodide for the same amount of time, and the size of the nuclei in Neo cells averaged 89 relative units larger in all three experiments.

Growth characteristics. To determine the doubling time, Neo and tMK cells were synchronized by growing them in the presence of 0.5% FBS for 48 h. The cells were then trypsinized and washed in medium containing 0.5% serum, and 50,000 Neo and tMK cells were plated in triplicate in 0.5% serum. After attachment, the cells were serum stimulated by raising the serum concentration to 10%. Cells were trypsinized at 0, 24, 48, and 72 h after serum stimulation and counted. A curve-fitting program was then used to determine the doubling time. Only the mean doubling time is reported in Table 1 because the curve-fitting program used to calculate the doubling time only considers the mean of data at each time point. Bromodeoxyuridine (BrDU) incorporation was quantified in cells that were synchronized and serum stimulated as described above. Cells were incubated with BrDU and stained with an antibody to BrDU, and positive cells were expressed as a percentage of total cells, as previously described (18).

MAP kinase assays. Cells synchronized and serum stimulated as described above were washed quickly in ice-cold PBS at various times and frozen on dry ice. Cells were extracted in ice-cold 1% Triton X-100, 5 mM EGTA, 5 mM $MgCl_2$, 1 mM

Table 1. *Characteristics of Neo and tMK cells*

	Neo	tMK
Myosin light chain phosphorylation, mol PO_4/mol light chain	0.20	0.96
Cell size, pl	3.2 ± 0.0	1.2 ± 0.03
Relative nuclear size,	428	345
Doubling time, h	27	48
BrDU incorporation, % of cells	37.7 ± 0.7	15.9 ± 1.3

Values are means or means ± SE. Myosin light chain phosphorylation data are from Ref. 33. Electronic cell sizing, relative nuclear size, doubling time, and bromodeoxyuridine (BrDU) incorporation were quantified as described in MATERIALS AND METHODS.

benzamidine, 1 mM DTT, 1 mM sodium vanadate, 10 mM sodium pyrophosphate, 10 μg/ml aprotinin, 10 μg/ml leupeptin, 2 μg/ml pepstatin A, and 40 mM HEPES (pH 7.5), as described (40). Thirty micrograms of each extract were boiled in SDS sample buffer, and the proteins were separated by SDS-PAGE, transferred to nitrocellulose, and probed with an antibody to extracellular signal-regulated kinase (ERK) 1 (no. 06-182, Upstate Biotechnology, Lake Placid, NY). The primary antibodies were visualized by incubation with peroxidase-labeled secondary antibodies and development of the color reaction. These primary antibodies primarily recognize ERK1, and developing the color reaction to visualize ERK2 obscured ERK1. Therefore, only ERK1 is shown (see Fig. 7). To quantify changes in MAP kinase activity, cells were extracted in nondenaturing buffer, MAP kinase was immunoprecipitated, and MAP kinase activity assays were performed using [γ-^{32}P]ATP and myelin basic protein (MBP) as substrate, as described (40). Aliquots of the reaction mixtures were analyzed by SDS-PAGE, and the bands representing the MBP were excised and counted. The translocation of MAP kinase was investigated by performing antibody immunofluorescence studies on cells plated on fibronectin-coated coverslips. These cells were synchronized and serum stimulated as described above. Cells were then fixed at *time zero* (no serum stimulation) and at 60 min after serum stimulation in freshly made 3% formaldehyde in PBS for 7 min and were permeabilized by incubation in 0.1% Triton X-100 and 0.1% deoxycholate in PBS for 7 min. MAP kinase was visualized using the same antibodies to ERK1 and ERK2 described above and a Texas red-labeled secondary antibody. The coverslips were mounted on slides and photographed using a Zeiss IM 35 inverted photomicroscope and a Planapo ×63, 1.4-numerical aperture objective.

Statistical analyses. The data were evaluated by Student's *t*-test and considered statistically significant when $P < 0.05$.

RESULTS

MLCK is a calcium/calmodulin-dependent enzyme that phosphorylates Ser-19 of the 20-kDa light chain of vertebrate smooth muscle and nonmuscle myosin II (1, 44). Myosin light chain phosphorylation stimulates the actin-activated ATPase activity of myosin II purified from smooth muscle and nonmuscle cells (1, 44). This reaction regulates smooth muscle contraction (9) and promotes the association of myosin II into filaments (43, 48). Proteolytic digestion of the purified enzyme (22) or insertion of a stop codon following Lys-793 (19) results in a truncated, constitutively active enzyme that maintains the specificity of the parent enzyme for Ser-19. Therefore, NIH/3T3 fibroblasts were transduced with retroviral vectors containing either the neomycin resistance gene and tMK (tMK cells) or the neomycin resistance gene alone (Neo cells) and selected in G418 (33). We previously reported that the stoichiometry of myosin light chain phosphorylation is increased in tMK cells compared with Neo cells (Table 1) and that this phosphorylation is confined to Ser-19 (33). Immunoprecipitation of myosin II from Neo and tMK cells labeled with ^{32}P performed throughout these experiments (Fig. 1) demonstrated increases in myosin light chain phosphorylation qualitatively similar to those previously reported (33).

The effects of increasing myosin light chain phosphorylation on cytoskeletal mechanics was studied using various assays. First, cortical tension was quantified directly by using a microprobe to deform the free surface of adherent cells (49). Mean cytoskeletal stiffness was increased almost 100% in tMK cells compared with Neo cells (Fig. 2). Okadaic acid (0.03–3.0 μM), a phosphatase inhibitor that increases myosin light chain phosphorylation (48), increased stiffness in a dose-dependent fashion in Neo cells (not shown), with the maximal effect observed at 3 μM. Okadaic acid had no effect on the stiffness of tMK cells, suggesting that cytoskeletal stiffness is near maximal in tMK cells. The combination of 3 μM okadaic acid and 3 μM cytochalasin D, which disrupts actin filaments (7), decreased stiffness in Neo cells to a very low level (Fig. 2). In contrast, stiffness remained elevated in tMK cells under similar conditions.

Cytoskeletal stiffness was also quantified by measuring the ability of cell surface receptor-bound magnetic beads to resist shear stresses applied using magnetic twisting cytometry (46). Beads coated with RGD peptide, which is a ligand for integrin receptors (46),

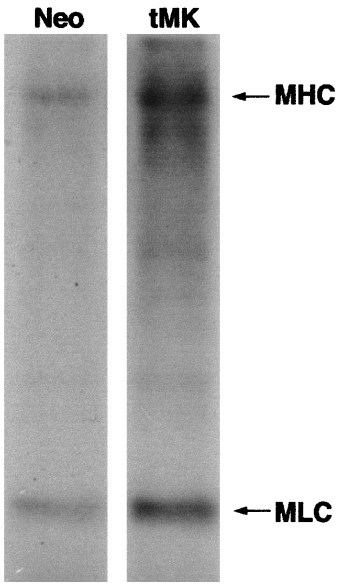

Fig. 1. Myosin light chain phosphorylation in Neo and tMK cells. Myosin was immunoprecipitated from Neo and tMK cells labeled with ^{32}P and analyzed by SDS-PAGE and autoradiography. Note marked increase in myosin light chain (MLC) phosphorylation in tMK cells compared with Neo cells. There was approximately the same amount of myosin heavy chain (MHC), as judged by Coomassie blue staining, in both lanes.

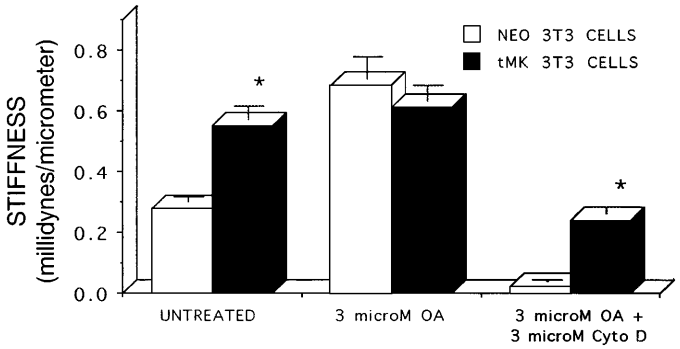

Fig. 2. Quantification of cytoskeletal stiffness by mechanical deformation. Mechanical deformation assays were performed on untreated cells, cells treated with 3 μM okadaic acid (OA), and cells treated with 3 μM okadaic acid and 3 μM cytochalasin D (Cyto D), as described in MATERIALS AND METHODS. Data are means ± SE; $n > 35$ cells in each group. *$P \leq 0.05$ compared with respective control.

showed ~50% increase in stiffness in tMK cells compared with Neo cells (Fig. 3). Okadaic acid also increased the twisting stiffness in Neo cells in a dose-dependent fashion (data not shown). Cytochalasin D treatment (3 μM, final) decreased twisting stiffness in both cell types (Fig. 3), indicating that the tMK effects on stiffness are mediated, at least in part, through an interaction with microfilaments. This conclusion is supported by the observation that the twisting of beads coated with AcLDL, a ligand for a transmembrane receptor that is not efficiently coupled to the cytoskeleton (46), was equally low in both cell types (Fig. 3).

We then investigated the ability of Neo and tMK cells to resist internal deformation by examining the responses of plated cells and cells in suspension to decreasing osmolarity. The responses of cells in monolayer were determined using an ECIS Biosensor (17) in which cells are plated in a well of a modified tissue culture dish that contains a small gold electrode and a counter electrode. A current passed across the gold electrode is restricted and eventually plateaus as the cells attach and form a confluent monolayer on the electrode. Cell contraction increases the dimensions of the paracellular spaces, thereby increasing current flow and decreasing resistance. Decreasing osmolarity is predicted to increase resistance by *1*) swelling the cells and thus increasing the thickness of the monolayer and *2*) decreasing the dimensions of the paracellular spaces, both of which impede current flow. Figure 4 shows that the peak resistance is greater in Neo cells at all osmolarities, as predicted for cells with a softer cytoskeleton. Moreover, at all osmolarities, there is a greater increase in peak resistance in Neo cells than in tMK cells (Fig. 4).

The responses of cells in suspension to decreasing osmolarity were determined by performing electronic cell sizing (34). Figure 5 shows that tMK cells in suspension are smaller in isosmolar medium than Neo cells, an observation that is consistent with an internal contraction of the cytoskeleton in tMK cells. Figure 5 also shows that tMK cells are much more resistant to osmotic swelling than are Neo cells and that Neo cells appear to lyse at a higher osmolarity than tMK cells. Thus tMK cells have a stiffer, more stable cytoskeleton than Neo cells (Figs. 2 and 3); this increase in cytoskeletal stiffness correlates with increased resistance to osmotic swelling (Figs. 4 and 5).

The effects of increasing myosin light chain phosphorylation on cell growth and division were studied next. Analysis of the growth rate showed that the doubling time is significantly increased in tMK cells compared with Neo cells (Fig. 6 and Table 1). In addition, more Neo cells than tMK cells were in S phase at 24 h following serum stimulation of synchronized cells as judged by BrDU incorporation (Table 1). Because cell size has been correlated with S phase entry and division (see DISCUSSION), we performed assays to quantify cell and nuclear size. Electronic cell sizing demonstrated that tMK cells in isotonic solution are smaller than Neo cells (Fig. 5 and Table 1). Time of flight measurements were also performed to compare the sizes of the nuclei in Neo and tMK cells. Although three

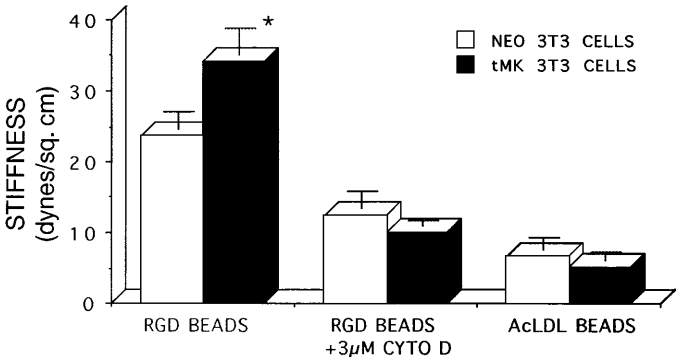

Fig. 3. Quantification of cytoskeletal stiffness by magnetic twisting cytometry. Magnetic twisting cytometry using RGD-coated beads in presence or absence of 3 μM cytochalasin D or beads coated with acetylated low-density lipoproteins (AcLDL) was performed as described in MATERIALS AND METHODS. Data are means ± SE; $n \geq 3$. *$P \leq 0.05$ compared with respective control.

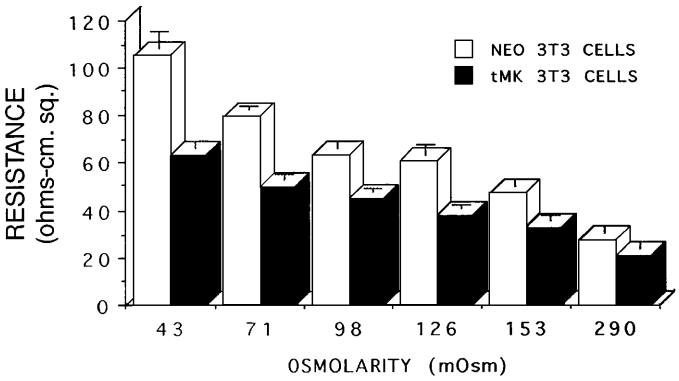

Fig. 4. Changes in electrical resistance in response to decreasing osmolarity in tMK and Neo cells grown in monolayers. Osmolarity was decreased sequentially, and peak electrical resistance was measured using an ECIS Biosensor. Note that resistance is higher and rises more rapidly in Neo cells than in tMK cells (means ± SE; $n \geq 4$ separate sets of cells). All values for tMK cells are significantly different ($P < 0.05$) from those for Neo cells at all osmolarities except 290 mosM.

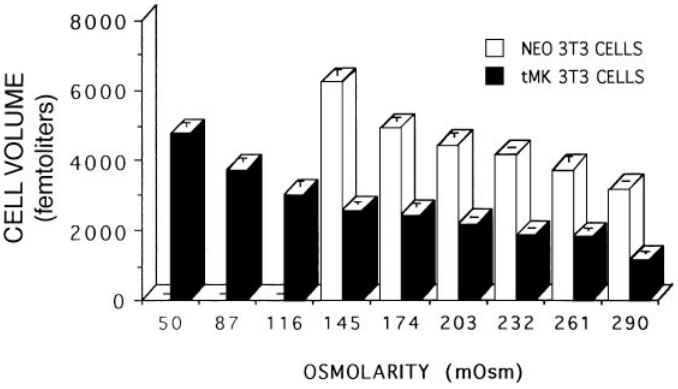

Fig. 5. Responses of Neo and tMK cells in suspension to decreasing osmolarity. Osmolarity of cells in suspension was decreased sequentially, and cell volume was quantified electronically (MATERIALS AND METHODS). No Neo cells were detected below 145 mosM, suggesting that cells had ruptured. Data are means ± SE; $n \geq 3$. All values for tMK cells are significantly different ($P < 0.05$) from those for Neo cells at all osmolarities.

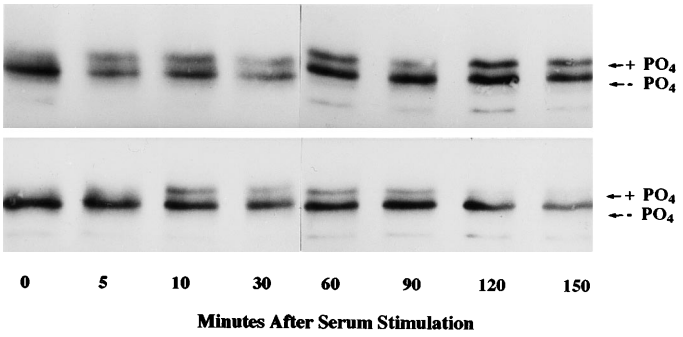

Fig. 7. Gel shift assay of mitogen-activated protein kinase (MAP kinase) activation in Neo (*top*) and tMK (*bottom*) cells. Synchronized Neo and tMK cells were stimulated with serum and analyzed as described in MATERIALS AND METHODS. Active, phosphorylated, and slower migrating form of MAP kinase, extracellular signal-regulated kinase (ERK) 1 ($+PO_4$), appears by 5 min in Neo cells, whereas it does not appear until 10 min after serum stimulation in tMK cells. Although only ERK1 is shown, developing color reaction longer showed a similar relationship for ERK2 in Neo and tMK cells. This experiment was repeated 3 times.

such experiments were performed, Table 1 shows the data from a single experiment because the time of flight gives a relative measure of nuclear size due to variability in the binding of propidium iodide to the DNA. Nevertheless, the nuclei in Neo cells averaged 89 relative units larger than those in tMK cells in all three experiments.

We then investigated whether the decrease of growth kinetics in tMK cells was associated with alterations in the activation of MAP kinase. Gel shift assays that are designed to detect the phosphorylated, activated forms of ERK1 and ERK2 showed that the activation of ERK1 (Fig. 7) and ERK2 (not shown) is slower in tMK cells than in Neo cells. The data also suggest that the rate of ERK dephosphorylation is also faster in tMK cells (Fig. 7). Phosphorylation assays (Fig. 8) performed on immunoprecipitated enzyme using MBP as a substrate confirmed that MAP kinase activation is retarded in tMK cells compared with Neo cells. Immunofluorescence assays were also performed because MAP kinase is known to translocate to the nucleus following mitogenic stimulation (5, 32, 40, 50). Figure 9 shows that the translocation of MAP kinase to the nucleus is retarded in tMK cells compared with Neo cells at 60 min after serum stimulation.

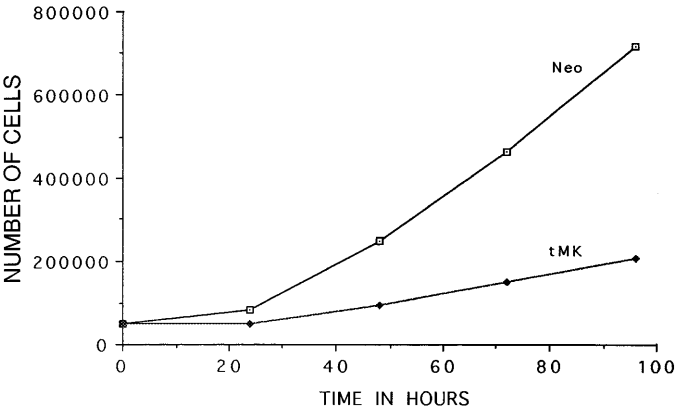

Fig. 6. Doubling time of Neo and tMK cells. Synchronized cells were trypsinized and counted, and equal numbers of cells were plated in triplicate as described in MATERIALS AND METHODS. Cells were then serum stimulated and counted at times shown. Data are means for triplicates from a single experiment, and tMK values at 24, 48, and 72 h are significantly different from those for Neo cells at same times.

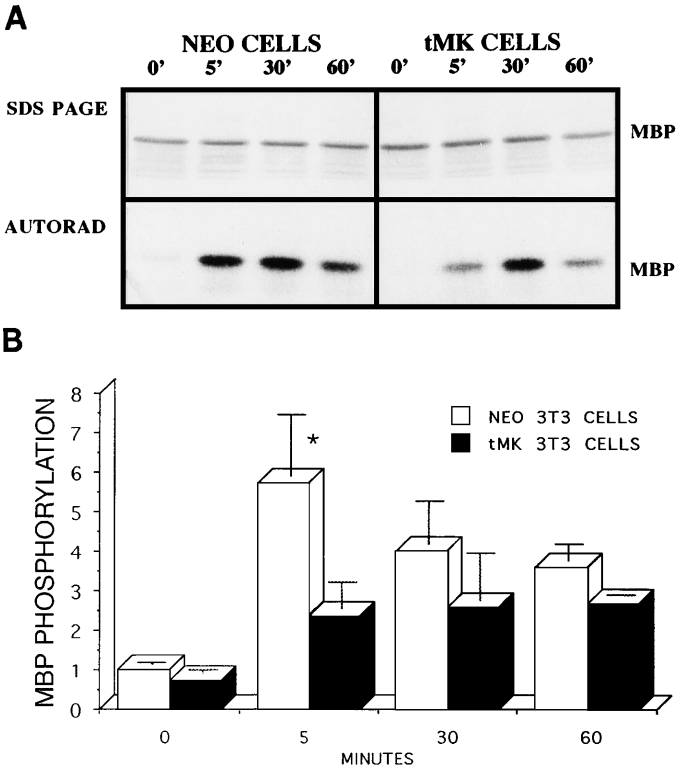

Fig. 8. MAP kinase activity assays. Synchronized Neo and tMK cells were stimulated with serum, MAP kinase was immunoprecipitated, and kinase activity was analyzed as described in MATERIALS AND METHODS using myelin basic protein (MBP) as substrate. *A*: Coomassie blue staining (SDS-PAGE) and autoradiogram (AUTORAD) of region of gel containing MBP. *B*: experiment in *A* was repeated 3 times, and aggregate data (means ± SE) from these experiments are shown. Data are expressed as increase in ^{32}P incorporation into MBP in terms of multiples of the level in Neo cells at *time 0*, which is set to 1. *Difference in MBP phosphorylation by Neo and tMK cells at 5 min after serum stimulation is statistically significant ($P < 0.05$).

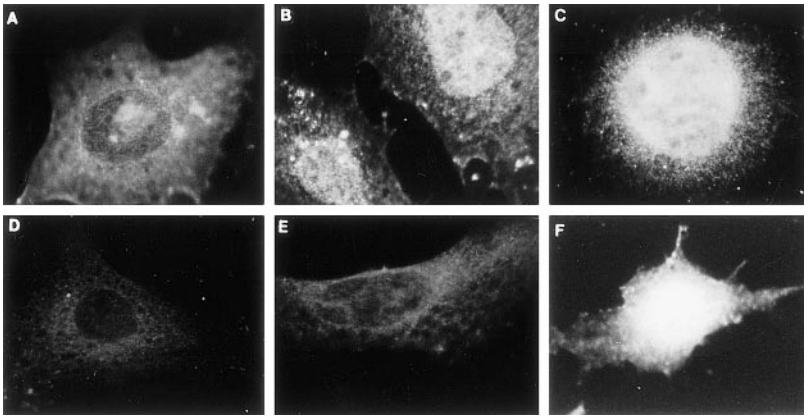

Fig. 9. Immunofluorescence localization of MAP kinase. Synchronized Neo (*A–C*) and tMK (*D–F*) cells before (*A* and *D*) and after 60 min (*B* and *E*) and 120 min (*C* and *F*) of serum stimulation were fixed and stained with antibodies to MAP kinase. Note nuclear staining in Neo cells (*B*) and absence of nuclear staining in tMK cells (*E*) at 60 min. All cells (100%) of both cell types contained nuclear staining at 120 min.

DISCUSSION

Inhibiting actin-myosin II interactions is known to decrease cytoskeletal stiffness. Experiments have shown that disrupting actin filaments with cytochalasin D decreases cytoskeletal stiffness as quantified by both mechanical deformation (49) and magnetic twisting cytometry (46). Similarly, cortical tension is lower in *Dictyostelium* amoebas lacking myosin II heavy chain (35). The implication of these data is that decreasing actin-myosin II interactions releases the internal tension generated by these proteins and makes the cytoskeleton less stiff. They also predict that the converse, namely increasing actin-myosin II interactions, should increase stiffness by generating a contractile tension within cells. This, in turn, leads to the hypothesis that myosin light chain phosphorylation, which regulates the actin-myosin II interaction in smooth muscle and nonmuscle cells (1, 9, 44), determines at least in part the stiffness of the cytoskeleton. This hypothesis is indirectly supported by the demonstration that vasoconstrictors and vasodilators that are known to modulate myosin light chain phosphorylation increase and decrease cytoskeletal stiffness, respectively, in smooth muscle cells (21). We tested this hypothesis by studying the mechanical properties of cells expressing the catalytic domain of MLCK. The data presented in Figs. 2–5 provide direct support for it.

The data in Figs. 4 and 5 also implicate myosin light chain phosphorylation in regulating cell swelling and support the hypothesis that the cytoskeleton acts as a resistive element to volume changes (3, 8, 31). Although volume regulation is a complex process, the cytoskeleton contributes to the cellular response to changes in osmolarity (3, 8, 31), and *Dictyostelium* resist volume changes in response to increasing osmolarity by redistributing their actin and myosin to the cortex (27). Other experiments have shown that muscle cells from MDX mice lacking dystrophin have a decreased stability in response to osmotic shock (30) compared with normal cells containing dystrophin. Mechanical deformation assays have also shown that muscle cells from MDX mice have a substantially lower stiffness than matched normal cells (30, 36). These studies demonstrate that decreasing stiffness by depleting the cortical cytoskeleton of specific structural proteins also results in a decrease in osmotic stability. Our data further support the hypothesis that the cytoskeleton resists volume changes (3, 8, 31), by demonstrating for the first time that cells with increased myosin light chain phosphorylation and a stiffer cytoskeletal are more resistant to osmotic swelling.

Our data also provide insights into how changes in the physical characteristics of the cytoskeleton affect cell growth and division. It is well known that actin and microfilaments are crucial for cell growth and cell division. Actin is considered an early response gene (11, 24), and actin-dependent morphological changes are among the earliest seen following growth factor or serum stimulation (20). In addition, growth factor stimulation or ligation of integrin receptors by extracellular matrix activates signaling pathways that result in MAP kinase activation and cytoskeletal changes, both of which are essential for G_0-to-G_1 transition (25). It is also known that cytochalasin D blocks MAP kinase activation and progression through the cell cycle (20). Thus decreasing cytoskeletal stiffness by disrupting the actin cytoskeleton blocks cell cycle progression. Similarly, our data show that increasing cytoskeletal stiffness (Figs. 2–5) also retards cell growth and cell division (Table 1 and Fig. 6). Moreover, the data suggest that both decreasing and increasing cytoskeletal tension alter the efficient transduction of signals that regulate cell growth, as indicated by delays in MAP kinase activation and extended doubling time (Figs. 7–9).

How changes in the mechanical properties of the cytoskeleton affect cell division is currently unclear. It is clear that the transition from interphase into M phase requires almost complete dissolution of all components of the cytoskeleton (2). Tubulin must subsequently reassemble into the spindle while actin and myosin II must congregate in the cleavage furrow before cytokinesis (2). This is a precise, highly regulated process. Disrupting this process by destabilizing actin filaments (20) or stabilizing microtubules (41) blocks mitosis. The implication is that disrupting the timing of these cytoskeletal changes can either block or retard mitosis. Our data demonstrate that tMK cells enter S phase more slowly (Table 1) and have longer doubling times than Neo cells (Fig. 6). While not

excluding other mechanisms, our data suggest that increasing myosin light chain phosphorylation prevents the timely dissolution of the cytoskeleton, perhaps in a manner that is analogous to the effect of taxol on cell division.

Another possibility is that cytoskeletal stiffness affects cell growth. Cells must grow by doubling their DNA and protein contents and duplicating their organelles before they can divide (2). Cell growth is profoundly affected by cell shape (37). Highly spread cells exhibit higher rates of DNA synthesis and cell division (14, 42). Cell spreading, in turn, appears to be controlled by the mechanical tension generated within the cytoskeleton by actin-myosin II interactions (23, 24, 41). The effect of spreading on DNA synthesis and cell division may be due to a direct effect of cytoskeletal mechanics on the nucleus. Maniotis et al. (29) demonstrated a direct connection between the cytoskeleton and the nucleus by showing that exerting mechanical force on cell surface integrin receptors changes the shape of the nucleus through the cytoskeleton. tMK cells have a stiffer cytoskeleton, are smaller, have smaller nuclei, enter S phase more slowly, and have more extended doubling times than Neo cells. When the data are considered in the context of the work described above (4, 14, 23, 24, 29, 41, 42), it seems possible that tMK cells take longer to enter the cell cycle and divide because tension generated by more actin-myosin II cross bridges retards both spreading and cell growth.

Our data also suggest a more complex role for myosin II in cell division than previously suspected. Myosin II has been localized in the cleavage furrow (15, 16) and shown to be essential for cytokinesis in metazoan cells. Classic experiments have shown that injecting an antibody to myosin II into starfish blastomeres blocks cytokinesis (28), whereas genetic manipulation of myosin II heavy chain expression in *Dictyostelium discoideum* results in multinucleated cells (10, 26). Myosin light chain phosphorylation has also been implicated in regulating the timing of cytokinesis (13, 38). It is possible that tMK cells divide more slowly because increasing myosin light chain phosphorylation retards the redistribution of myosin II to the cleavage furrow before cytokinesis. At the same time, the observations that MAP kinase activation, S phase entry, and doubling time are altered in tMK cells suggest that myosin II is involved in cell growth and division in multiple, complex ways in addition to mediating cytokinesis.

In conclusion, we used multiple approaches to obtain the most compelling data to date that myosin light chain phosphorylation regulates the mechanical characteristics of the cytoskeleton. Our data also provide important support for the idea that the cortical cytoskeleton is the major barrier to osmotic swelling in mammalian cells. In addition, the data demonstrate that changes in myosin light chain phosphorylation affect the kinetics of MAP kinase activation and progression through the cell cycle. Our current working hypothesis is that the plasticity of the cytoskeleton is regulated in great part by changes in the level of myosin light chain phosphorylation and that changes in myosin light chain phosphorylation affect signal transduction pathways by altering the mechanical properties of the cytoskeleton. This hypothesis predicts that decreasing myosin light chain phosphorylation will soften the cytoskeleton and make the cells more susceptible to osmotic swelling and other types of physical deformation. We also anticipate that decreasing myosin light chain phosphorylation will alter cell cycle progression. These possibilities require investigation.

We thank Asra Malik for the use of his ECIS Biosensor.

This research was supported by National Institutes of Health (NIH) Grants HL-45674 (to M. E. O'Donnell), HL-33009 (to N. Wang), CA-45548 (to D. Ingber), GM-38838 (to E. Elson), and HL-02411 and HL-59618 (to P. de Lanerolle) and by the Harriet Brooks Fund of the University of Illinois at Chicago. S. Cai and L. Pestic-Dragovich were supported by NIH Training Grant HL-076922.

This work was done during P. de Lanerolle's tenure as the Florence and Arthur Brock Established Investigator of the Chicago Lung Association.

Address for reprint requests: P. de Lanerolle, Dept. of Physiology and Biophysics, University of Illinois at Chicago, 835 S. Wolcott, Chicago, IL 60612.

Received 26 March 1998; accepted in final form 21 July 1998.

REFERENCES

1. **Adelstein, R. S.** Regulation of contractile proteins by phosphorylation. *J. Clin. Invest*. 72: 1863–1866, 1983.
2. **Alberts, B., D. Bray, J. Lewis, M. Raff, K. Roberts, and J. D. Watson.** *The Molecular Biology of the Cell* (3rd ed.). Hamden, CT: Garland, 1994, p. 911–946.
3. **Cantiello, H. F., A. G. Prat, J. V. Bonventre, C. C. Cunningham, J. H. Hartwig, and D. A. Ausiello.** Actin-binding protein contributes to cell volume regulatory ion channel activation in melanoma cells. *J. Biol. Chem*. 268: 4596–4599, 1993.
4. **Chen, C. S., M. Mrksich, S. Huang, G. M. Whitesides, and D. E. Ingber.** Geometric control of cell life and death. *Science* 276: 1425–1428, 1997.
5. **Chen, Q., M. S. Kinch, T. H. Lin, K. Burridge, and R. L. Juliano.** Integrin-mediated cell adhesion activates mitogen-activated protein kinases. *J. Biol. Chem*. 269: 26602–26605, 1994.
6. **Chrzanowska-Wodnicka, M., and K. Burridge.** Rho-stimulated contractility drives the formation of stress fibers and focal adhesions. *J. Cell Biol*. 133: 1403–1415, 1996.
7. **Cooper, J. A.** Effects of cytochalasin and phalloidin on actin. *J. Cell Biol*. 105: 1473–1477, 1987.
8. **Cornet, M., I. H. Lambert, and E. K. Hoffmann.** Relation between cytoskeleton, hypo-osmotic treatment and volume regulation in Erlich ascites tumor cells. *J. Membr. Biol*. 131: 55–66, 1993.
9. **De Lanerolle, P., and R. J. Paul.** Myosin phosphorylation/dephosphorylation and regulation of airway smooth muscle contractility. *Am. J. Physiol*. 261 (*Lung Cell. Mol. Physiol*. 5): L1–L14, 1991.
10. **De Lozanne, A., and J. A. Spudich.** Disruption of the *Dictyostelium* myosin heavy chain gene by homologous recombination. *Science* 236: 1086–1091, 1987.
11. **Elder, P. K., L. J. Schmidt, T. Ono, and M. J. Getz.** Specific stimulation of actin gene transcription by epidermal growth factor and cycloheximide. *Proc. Natl. Acad. Sci. USA* 81: 7474–7480, 1984.
12. **Elson, E. L.** Cellular mechanics as an indicator of cytoskeletal structure and function. *Annu. Rev. Biophys. Biophys. Chem*. 17: 397–430, 1988.
13. **Fishkind, D. J., L.-G. Cao, and Y.-L. Wang.** Microinjection of the catalytic fragment of myosin light chain kinase into dividing cells: effects on mitosis and cytokinesis. *J. Cell Biol*. 114: 967–975, 1991.
14. **Folkman, J., and A. Moscona.** Role of cell shape in growth control. *Nature* 273: 345–349, 1978.

15. **Fujiwara, K., and T. D. Pollard.** Fluorescent antibody localization of myosin in the cytoplasm, cleavage furrow and mitotic spindle of human cells. *J. Cell Biol*. 71: 848–875, 1976.
16. **Fukui, Y., T. J. Lynch, H. Brzeska, and E. D. Korn.** Myosin I is located at the leading edges of locomoting *Dictyostelium* amoebae. *Nature* 341: 328–331, 1989.
17. **Giaever, I., and C. R. Keese.** A morphological biosensor for mammalian cells. *Nature* 366: 591–592, 1993.
18. **Gratzner, H. G.** Monoclonal antibody to 5-bromo and 5-iododeoxyuridine: a new reagent for detection of DNA replication. *Science* 218: 474–475, 1982.
19. **Guerriero, V., Jr., M. A. Russo, N. J. Olson, J. A. Putkey, and A. R. Means.** Domain organization of chicken gizzard myosin light chain kinase deduced from cloned cDNA. *Biochemistry* 25: 8372–8381, 1986.
20. **Hall, A.** Rho GTPases and the actin cytoskeleton. *Science* 279: 509–514, 1998.
21. **Hubmayr, R. D., S. A. Shore, J. J. Fredberg, E. Planus, R. A. Panettieri, Jr., W. Moller, J. Heyder, and N. Wang.** Pharmacological activation changes stiffness of cultured human airway smooth muscle cells. *Am. J. Physiol*. 271 (*Cell Physiol*. 40): C1660–C1668, 1996.
22. **Ikebe, M., M. Stepinska, B. E. Kemp, A. R. Means, and D. J. Hartshorne.** Proteolysis of smooth muscle myosin light chain kinase. *J. Biol. Chem*. 260: 13828–13834, 1987.
23. **Ingber, D. E., D. Prusty, Z. Sun, H. Batensky, and H. Wang.** Cell shape, cytoskeletal mechanics and cell cycle control in angiogenesis. *J. Biomech*. 28: 1471–1484, 1995.
24. **Jamal, S., and E. Ziff.** Transactivation of c-fos and β-actin genes by raf as a step in early response to transmembrane signals. *Nature* 344: 463–466, 1990.
25. **Joneson, T., M. A. White, M. H. Wigler, and D. Bar-Sagi.** Stimulation of membrane ruffling and MAP kinase activation by distinct effectors of RAS. *Science* 271: 810–812, 1996.
26. **Knecht, D. A., and W. F. Loomis.** Antisense RNA inactivation of myosin heavy chain gene expression in *Dictyostelium discoideum*. *Science* 236: 1081–1086, 1987.
27. **Kuwayama, H., M. Ecke, G. Gerisch, and P. J. M. Van Haastert.** Protection against osmotic stress by cGMP-mediated myosin phosphorylation. *Science* 271: 207–209, 1996.
28. **Mabuchi, I., and M. Okuno.** The effect of myosin antibody on the division of starfish blastomeres. *J. Cell Biol*. 74: 251–263, 1977.
29. **Maniotis, A., C. Chen, and D. E. Ingber.** Demonstration of mechanical connections between integrins, cytoskeletal filaments and nucleoplasm that stabilize nuclear structure. *Proc. Natl. Acad. Sci. USA* 94: 849–854, 1997.
30. **Menke, A., and B. Jokusch.** Decreased osmotic stability of dystrophin-less muscle cells from MDX mouse. *Nature* 349: 69–71, 1991.
31. **Mills, J. W., E. M. Schwiebert, and B. A. Stanton.** In: *Cellular and Molecular Physiology of Volume Regulation*, edited by K. Strange. Boca Raton, FL: CRC, 1994, p. 241–258.
32. **Morino, N., T. Mimura, K. Hamasaki, K. Tobe, K. Ueki, K. Kikuchi, K. Takehara, T. Kadowaki, Y. Tazaki, and Y. Nojima.** Matrix/integrin interaction activates the mitogen activated protein kinase $p44^{erk-1}$ and $p42^{erk-2}$. *J. Biol. Chem*. 270: 269–273, 1995.
33. **Obara, K., G. Nikcevic, L. Pestic, G. Nowak, D. D. Lorimer, V. Guerriero, E. L. Elson, R. J. Paul, and P. de Lanerolle.** Fibroblast contractility without an increase in basal myosin light chain phosphorylation in wild type cells and cells expressing the catalytic domain of myosin light chain kinase. *J. Biol. Chem*. 270: 18734–18737, 1995.
34. **O'Donnell, M. E.** Role of Na-K-Cl cotransport in vascular endothelial cell volume regulation. *Am. J. Physiol*. 264 (*Cell Physiol*. 33): C1316–C1326, 1993.
35. **Pasternak, C., J. A. Spudich, and E. L. Elson.** Capping of surface receptors and concomitant cortical tension are generated by conventional myosin. *Nature* 341: 549–551, 1989.
36. **Pasternak, C., and E. L. Elson.** Mechanical function of dystrophin in muscle cells. *J. Cell Biol*. 128: 355–361, 1995.
37. **Roushlati, E.** Stretching is good for a cell. *Science* 276: 1345–1346, 1997.
38. **Satterwhite, L. L., M. J. Lohka, K. L. Wilson, T. Y. Scherson, L. J. Corden, J. L. Cisek, and T. D. Pollard.** Phosphorylation of myosin-II regulatory light chain by cyclin-$p34^{cdc2}$: a mechanism for the timing of cytokinesis. *J. Cell Biol*. 118: 595–605, 1992.
39. **Schiff, P. B., J. Fant, and S. B. Horwitz.** Promotion of microtubule assembly, in vitro, by taxol. *Nature* 277: 665–667, 1979.
40. **Seger, R., D. Seger, A. A. Reszka, E. S. Munar, H. Eldar-Finkelman, G. Dobrowolska, A. M. Jensen, J. S. Campbell, E. H. Fischer, and E. G. Krebs.** Over-expression of mitogen-activated protein kinase kinase (MAPKK) and its mutants in NIH 3T3 cells. *J. Biol. Chem*. 269: 25699–25709, 1994.
41. **Sims, J. R., S. Karp, and D. E. Ingber.** Altering the cellular mechanical force balance results in integrated changes in cell, cytoskeletal and nuclear shape. *J. Cell Sci*. 103: 1215–1222, 1992.
42. **Singhvi, R., A. Kumar, G. P. Lopez, G. N. Stephanopoulos, D. I. C. Wang, G. M. Whitesides, and D. E. Ingber.** Engineering cell shape and function. *Science* 264: 696–698, 1994.
43. **Trybus, K. M., T. W. Huiatt, and S. Lowey.** A bent monomeric conformation of myosin from smooth muscle. *Proc. Natl. Acad. Sci. USA* 79: 6151–6155, 1982.
44. **Trybus, K. M.** Myosin regulation and assembly. In: *Biochemistry of Muscle Contraction*, edited by M. Barany. San Diego, CA: Academic, 1996, p. 37–46.
45. **Vindelov, L. L., J. Christensen, and N. I. Nissen.** A detergent-trypsin method for the preparation of nuclei for flow cytometric DNA analysis. *Cytometry* 3: 323–327, 1983.
46. **Wang, N., J. P. Butler, and D. E. Ingber.** Mechnotransduction across the cell surface and through the cytoskeleton. *Science* 260: 1124–1127, 1993.
47. **Wilson, A. K., G. Gorgas, W. D. Claypool, and P. de Lanerolle.** An increase or a decrease in myosin II phosphorylation inhibits macrophage motility. *J. Cell Biol*. 114: 277–283, 1991.
48. **Wilson, A. K., A. Takai, J. C. Ruegg, and P. de Lanerolle.** Okadaic acid, a phosphatase inhibitor, decreases macrophage motility. *Am. J. Physiol*. 260 (*Lung Cell. Mol. Physiol*. 4): L105–L112, 1991.
49. **Worthen, G. S., B. Schwab III, E. L. Elson, and G. P. Downey.** Mechanics of stimulated neutrophils: cell stiffening induced retention in capillaries. *Science* 245: 183–186, 1989.
50. **Zhu, X., and R. K. Assoian.** Integrin-dependent activation of MAP kinase: a link to shape-dependent cell proliferation *Mol. Biol. Cell* 6: 273–282, 1995.